

Design analysis and simulation of an external helical gear

Jinlong Yang¹, Kwang-Hee Lee¹ and Chul-Hee Lee^{1*}

Received: 18 Oct. 2023, Accepted: 17 Nov. 2023

Key Words: Helical gear pump, Parametric analysis, Rotor shape, Axial force, TwinMesh, CFX

Abstract: This study optimized the parameters of the helical gear based on the original external meshing helical gear pump, combined with the analysis of the stability and flow of the basic parameters of the equipment; herringbone gears were used to eliminate the axial force generated by the helical gears. An optimized helical gear rotor was built with NX. The error between the simulation and calculation results of pump displacement was 3.95% and the simulation results were valid. Analysis of the outlet pressure and lift changes (maximum change rates of 0.38% and 0.25%), pressure analysis of the XY center plane at different times in the same cycle (no pressure surge or drop), and analysis of the axial force of the primary and driven rotors (axis The axial force is close to 0) were performed. The results showed that the flow pulsation of the external gear pump was slight, the operation was smooth, vibration and friction were reduced, the wear of bearings and other components could be diminished, and the service life of the equipment was extended. The simulation results showed that the external gear pump met the design requirements.

Nomenclature

b: tooth width
 Ω : angular velocity of gear rotation
 R_a : spur gear addendum circle radius
 R_w : pitch circle radius
 R_b : base circle radius
 Φ : gear rotation angle
 f : distance between the meshing point and node
 Θ : rotation angle
 x : engh of the end face
 β : helix angle
 $q_{v \max}$: maximum value of the instantaneous flow rate
 $q_{v \min}$: minimum value of the instantaneous flow rate
 q_{vt} : theoretical flow rate
 \bar{q}_v : average flow rate
 ε : overlap coefficient of gear meshing
 r_j : pitch of the base circle
 Z : number of teeth
 m_t : end modulus
 m_n : normal modulus
 q : rated displacement
 f_t : tooth height coefficient

α_t : end face pressure angle
 v : average fluid velocity
 D : hydraulic diameter
 ν : fluid kinematic viscosity
 Φ : general scalar

1. Introduction

A pump is a machine that transports fluid or pressurizes a fluid. Its primary function is to transfer energy to the liquid to increase the power of a liquid. Pumps are used widely in water supply systems, agricultural irrigation, urban flood drainage, and other fields. Pumps are divided into three categories according to the working principle: positive displacement pump¹⁾, impeller pump²⁾, and other types of pumps³⁾. Among them, the positive displacement pump is the pump of using the change in the volume of the pump cylinder to transport liquid, mainly including screw pumps, plunger pumps, and gear pumps. For example, the gear pump has the features of low price, high reliability, and convenient maintenance, so the gear pump has been widely used, particularly the external gear pump is used more widely.

External meshing spur gear pumps have problems⁴⁾, such as radial force imbalance, bearing wear, and limited increase in working pressure. The reason is that spur gear meshes are line meshing. The tooth width line enters meshing simultaneously, and there will be a shock, which will cause vibration and noise during the transmission process. In addition, when the helical gear meshes, the point meshing changes gradually to coin meshing. The meshing line changes from short to long and then from long to short. This continuous change process can reduce

* Corresponding author: chulhee@inha.ac.kr

¹ Department of Mechanical Engineering, Inha University, Incheon 22212, Korea

Copyright © 2021, KSFC

This is an Open-Access article distributed under the terms of the Creative Commons Attribution Non-Commercial License (<http://creativecommons.org/licenses/by-nc/3.0>) which permits unrestricted non-commercial use, distribution, and reproduction in any medium, provided the original work is properly cited.

the impact and noise generated during operation, making the pump run more smoothly. Helical gears have a higher contact ratio than spur gears, which can achieve efficient transmission and help improve pump efficiency⁵⁾. The shape of helical gears is beneficial for distributing the pressure more evenly on the gear teeth, reducing the high-pressure area to improve the ability of a pump to handle high pressures and, at the same time, reduce noise and wear. The helical tooth shape of the helical gear can reduce the pulsation of fluid flow⁶⁾.

The shape of the rotor dramatically influences the performance of the helical gear pump⁷⁾, and many scholars have explored this aspect. A gear transmission device that eliminates low-frequency and large-amplitude flow pulsations generated by non-circular rotors is proposed by T Liu D et al.⁸⁾. Xuegang Z et al.⁹⁾ proposed a new type of external gear pump with a curved cylindrical gear as the rotor to solve cavitation. Zhao X et al.¹⁰⁾ designed a hydraulic gear pump with low/no surge fluid delivery and shallow noise emission levels. The common feature of the above studies is to solve specific problems by optimizing the design of a particular part of the helical gear pump. On the other hand, there needs to be more overall consideration, particularly the working environment and actual user requirements. Therefore, starting from the working environment and exact use requirements, this research redesigned the shape of the rotor from an overall perspective through parameter research, shape optimization, and engineering practice experience. To meet the needs of urban drainage, this type of pump should have a large displacement, high power, compact structure, and high reliability. The rotor shape of the external gear pump needs to be specifically designed to meet the requirements of use. Hence, its feasibility has been determined using a commercial CFD software simulation.

2. Analysis of primary influencing parameters

2.1 Flow pulsation coefficient

When the hydraulic pump is working, the change in instantaneous flow rate is uneven and changes with time. The change rule of the rapid flow rate per revolution is the same, called the flow pulsation of a hydraulic pump. Flow pulsation will affect the stability of the working parts of the pump body, causing pressure changes in the cavity and resulting in vibration and noise. The size of the flow pulsation is represented by the flow pulsation coefficient, which is also an important parameter to evaluate the external gear pump. The driving and driven wheels are a pair of involute gears with the same number of teeth, and the instantaneous flow rate of the external meshing spur gear pump¹¹⁻¹²⁾ can be expressed as follows:

$$q_{vs} = b\omega(R_a^2 - R_w^2 - R_b^2\Phi^2) \quad (1)$$

where b is the tooth width; ω is the angular velocity of gear rotation; R_a , R_w , and R_b are the spur gear addendum circle radius, pitch circle radius, and base circle radius, respectively, and Φ is the gear rotation angle.

Regarding the instantaneous flow rate of the external mesh helical gear pump¹³⁾, the helical gear can be divided into an equal parts (n represents the number of parts that the helical gear is divided into equivalent spur gears, which is the identical replacement method for calculating the transient flow rate of the helical gear.). Each piece can be equivalent to a spur gear, so its mathematical expression can be expressed as

$$q_{vh} = \sum_{i=0}^{n-1} \omega [(R_a^2 - R_w^2 - f^2(\theta + \frac{x \tan \beta}{nR})^2] \frac{b}{n} \quad (2)$$

where f is the distance between the meshing point and the node; θ is the rotation angle with the meshing point of the same gear on the reference plane; x is the length of the equipment end face, $x=ib$; β is the helix angle.

The flow pulsation coefficient can be defined in two ways:

$$\varphi = \begin{cases} \frac{q_{v \max} - q_{v \min}}{q_{vt}} \\ \frac{q_{v \max} - q_{v \min}}{q_v} \end{cases} \quad (3)$$

where $q_{v \max}$ is the maximum value of the instantaneous flow rate and $q_{v \min}$ is the minimum value of the instantaneous flow rate; q_{vt} is the theoretical flow rate;

\bar{q}_v is the average flow rate, and the half of the sum of $q_{v \max}$ and $q_{v \min}$ is its value.

Mathematical expression of theoretical flow is

$$q_{vt} = \sum_{i=0}^{n-1} \omega [R_a^2 - R_w^2 - \frac{K_v r_j}{12} (\theta + \frac{i \tan \beta}{nR})^2] \frac{b}{n} \quad (4)$$

where $K_v = 3\epsilon^2 - 6\epsilon + 4$, ϵ is the overlap coefficient of gear meshing.

The instantaneous flow is smallest when the gear starts to engage, or the engagement is about to end; the rapid flow is the largest at the meshing point. Referring to the derivation process and analysis of influencing factors of the flow pulsation coefficient by Liu Kun et al.¹⁴⁾, the value range of f is $(-\epsilon r_j / 2, \epsilon r_j / 2)$, where r_j is the pitch of the base circle. When $f = -\epsilon r_j / 2$ (or $f = \epsilon r_j / 2$), the minimum instantaneous flow is

$$q_{v \min} = \sum_{i=0}^{n-1} \omega [R_a^2 - R_w^2 - \frac{i^2 r_j^2}{4} (\theta + \frac{i \tan \beta}{nR})^2] \frac{b}{n} \quad (5)$$

When $f = 0$, the maximum instantaneous flow rate is

$$q_{v \max} = \sum_{i=0}^{n-1} \omega (R_a^2 - R_w^2) \frac{b}{n} \quad (6)$$

Combining Equations (3), (4), (5) and (6), we can get:

$$\varphi = \frac{\varepsilon^2 r_j^2 (\theta + \frac{ib \tan \beta}{nR})^2}{2[R_a^2 - R_w^2 - \frac{Kv r_j}{12} (\theta + \frac{ib \tan \beta}{nR})^2]} \quad (7)$$

where $r_j = m_n \pi \cos \alpha_n$; m_n is the normal modulus; $R_a = m_t Z + 0.5h$, where Z is the number of teeth; m_t is the end modulus; $h = R_a - R_w$ and $R = m_t Z$.

Equation (7) shows that the flow pulsation coefficient is related to the helix angle β . Zhang Jing et al.¹⁴⁾ used MATLAB software to program equation (7) to calculate the relationship between the flow pulsation coefficient and the helix angle of the helical gear. According to the results, when the tooth width is constant, the flow pulsation coefficient is inversely proportional to the helix angle. Therefore, in the design process of the external helical gear, obtaining a stable flow can be realized by changing the helix angle. On the other hand, a larger helix angle is better. According to engineering practice, the helix angle β is generally 8° to 25° ¹⁵⁾. The reason is that increasing the helix angle will increase the axial force and cause an imbalance during operation.

2.2 Main structural parameters

In urban flood drainage, pump displacement is essential to the rescue progress. The rated displacement (q) is related to the modulus of the end face (m_t), the teeth number (Z), the width of tooth (b), and the pressure angle. Its relationship satisfies equation (8)^{14,16)}

$$q = m_t^2 b \left\{ 2\pi \left(\frac{Z}{2} + f_t \right)^2 - Z^3 \left[2 - \cos \left(\frac{\pi}{2Z} \right) \sin \frac{\pi}{2Z} \right] \right\} \times 10^3 \quad (8)$$

where q is the helical gear hydraulic pump's rated displacement; f_t is the tooth height coefficient; $f_t = (\pi \cos \alpha_t)/4$, α_t is the end face pressure angle.

(1) Modulus

The modulus of the helical gear includes the end modulus (m_n) and the standard modulus (m_t). The average modulus is related to the processing of the bag, and the end modulus specifically determines the structural parameters of the equipment. Regardless of the average modulus, according to formula (8), the rated displacement (q) is proportional to the square of the end modulus (m_t). Therefore, an increase in the end modulus value method will increase the rated displacement. When the rated removal is constant, an increase in the modulus of the end face can allow a decrease in the number of gear teeth. The compact and lightweight design requirements determine the relationship between the number of teeth and the size of the external gear pump when the rated displacement is constant, as shown in Figure 1.

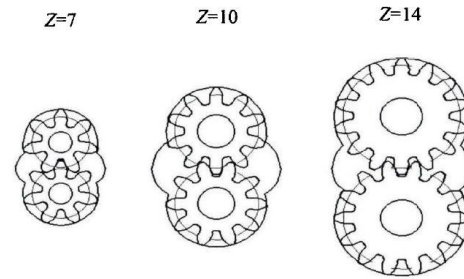


Fig. 1 Effect of number of teeth on gear pump size.²¹⁾

In urban drainage, when meeting the actual needs, a small and light external gear pump can adapt to a narrower working environment and a lower water level, which is convenient to move and reduce personnel dependence, and can complete drainage more efficiently. Therefore, the modulus of the end face and the modulus of the gear can be increased as much as possible during the design process. On the other hand, the number of teeth cannot be infinitely small because too few teeth are prone to undercutting during processing, which is not conducive to manufacturing.

(2) Number of teeth

According to formula (8), the number of teeth is positively correlated with the displacement when the modulus of the end face is constant. According to the relevant literature and combined engineering experience, the number of teeth (Z) of the external mesh helical gear low-pressure pump is 13–19, and the number of teeth (Z) of the high-pressure pump is 6–13. The number of teeth should be determined comprehensively in terms of flow rate, pulsation coefficient, and mechanical transmission efficiency. A decrease in the number of teeth is conducive to improving the transmission efficiency, but the flow pulsation will increase.

(3) Gear face pressure angle

Huang K J et al.¹⁷⁾ examined the relationship between the gear face pressure angle α_t (12° – 30°) and the maximum output flow rate and flow pulsation coefficient. The research results show that the maximum output flow increases as the gear face pressure angle α_t increases, but the flow pulsation coefficient decreases. Therefore, the gear face pressure angle should be increased as much as possible to meet the design requirements in the external gear pump design process. On the other hand, the friction force will increase if the gear face pressure angle is too large, and the transmission efficiency will be reduced. According to engineering practice experience and related research, the value of gear face pressure angle is generally 14.5° , 20° , 30° , and 35° .

(4) Tooth width

According to formula (8), the available tooth width (b) and rated displacement (q), end modulus (m_t), number of teeth (Z), and end pressure angle (α_t) satisfy the following relationship:

$$b = \frac{q}{m_t^2 \left\{ 2\pi \left(\frac{Z}{2} + f_t \right)^2 - Z^3 \left[2 - \cos \left(\frac{\pi}{2Z} \right) \sin \frac{\pi}{2Z} \right] \right\}} \times 10^3 \quad (9)$$

According to equation (9), the rated displacement is proportional to the tooth width when the modulus of the gear face, the number of teeth, and the coefficient of tooth height are constant. Therefore, the rated displacement of the external gear pump can be increased by increasing the tooth width when the modulus of the gear face, the number of teeth, and the tooth height coefficient are determined. As the tooth width increases, however, the maximum radial force and torque increase nonlinearly, and the axial force decreases nonlinearly¹⁸. Other parameters (such as dimensional tolerance and axial clearance) will also have a particular impact on the performance of the external mesh helical gear pump, and they will be considered when designing the outer gear pump rotor shape.

3. Gear rotor design analysis

3.1 Tooth profile

Regarding the analysis results of the main influencing parameters, the optimal design was determined based on the original helical gear to meet the needs of external gear pumps for rapid drainage in the event of urban floods and to achieve the design goals of low-flow pulsation, high pressure, and high lift. Figure 2 shows the 3D model of the external mesh helical pump gear before improvement. In actual use, problems include significant vibration and noise, low outlet pressure, and low lift. To solve these problems, optimize the design of the gear structure and use NX for digital modeling. According to engineering practice experience, analysis results, and parameter reference design value range, each parameter was corrected to meet the actual use requirements. Figure 3 shows a 3D model of the improved external mesh helical gear pump gear.

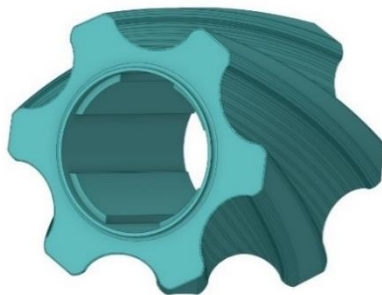


Fig.2 3D model of external mesh helical gear pump gear before improvement.

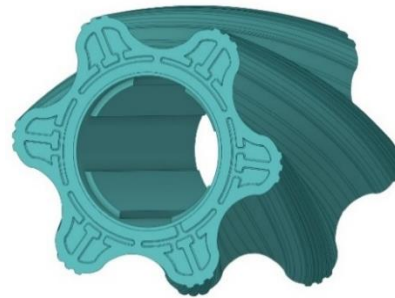


Fig. 3 Optimized 3D model of the external mesh helical gear pump gear.

3.2 Axial force

Helical gears run smoother and quieter than spur gears. On the other hand, a force perpendicular to the plane of the orbit of the equipment and parallel to the axis of the process will be generated during the rotation of the helical gear. This force is called axial force. The axial force will accelerate the wear and damage of bags. So, the design process should consider weakening or elimination of axial force. Mounting thrust bearings on one or both sides of the gear is a standard treatment. Because the thrust bearing can bear the axial load, the axial force is transmitted to the bearing instead of directly acting on the gear, reducing the damage of the axial force to the equipment. During the design process of the rotor structure, the axial force can be weakened using herringbone gears. Herringbone gears allow a compact construction, strong bearing capacity, stable operation, and small axial force. They are used widely on high-speed and heavy-duty occasions. Two helical gears have opposite rotation directions on both sides of the shaft. Due to opposite directions of rotation, axial forces generated on both sides of the shaft are equal in magnitude and opposite in direction. They cancel each other out through the shaft, and the bearing is not subject to axial force.

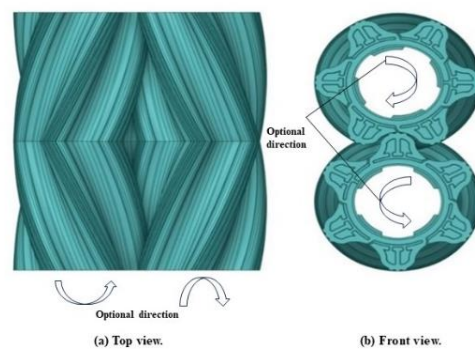


Fig. 4 Schematic diagram of herringbone gear transmission.

4. Simulation analysis

Table 1 Parameter table of the gear pump.

Name	Numerical value
Rated speed (RPM)	300
Tooth number	6
Tooth width (mm)	478
Addendum diameter (mm)	210.52
Gear center distance (mm)	180

Computational fluid dynamics (CFD) is the science of quantitatively predicting fluid flow phenomena with the aid of digital computers based on the three conservation laws (Conservation of mass, Momentum and Energy) that govern fluid motion. Compared with traditional experimental technology, it can obtain accurate data inside the fluid, such as pressure, velocity, temperature, and turbulence, which are challenging to obtain experimentally. In addition, it has high cost-effectiveness, shortened development cycle, strong visualization, and convenient design optimization. Utilize TwinMesh in conjunction with ANSYS CFX to complete the simulation and analysis of an external gear pump. The parameters of the gear pump are shown in Table 1.

4.1 Basics of fluid dynamics analysis

(1) Flow type

Flow is divided into laminar and turbulent flow. Laminar flow means that some fluids flow slowly during the flow process, and there will be stratified flow without mixing. Turbulent flow means some fluids flow fast; the streamlines cannot be clearly distinguished, and many eddies exist. Generally, the critical flow state of the liquid is determined by the Reynolds, which can be expressed as

$$Re = \frac{vD}{\nu} \tag{10}$$

where v is the average velocity of fluid; D is the hydraulic diameter; ν is the kinematic viscosity of fluid.

$Re \leq 2300$ is laminar flow. $Re \geq 8000-12000$ is turbulent flow. When $2300 \leq Re \leq 8000$, the fluid flow is in the transition zone between laminar and turbulent flow. Many simulation analyses and experimental verifications have been carried out on selecting the flow type of the external gear pump¹⁹⁾, and the flow is turbulent flow due to the strong shear in the transmission area and the suction chamber²⁰⁾.

(1) Turbulence model

Commonly used turbulence models include the standard $\kappa-\epsilon$ model, the Renormalization Group (RNG) $\kappa-\epsilon$ model, $\kappa-\omega$ model, and Shear-Stress Transport (SST) $\kappa-\omega$ model. The choice of turbulence model²¹⁾ affects the accuracy and reliability of the simulation results, affecting pump design and optimization. Regarding the standard $\kappa-\epsilon$ model, it ignores the effect of molecular viscosity and assumes that the flow is entirely turbulent. Hence, it is only suitable for simulating thoroughly turbulent flow.

The RNG $\kappa-\epsilon$ model improves the standard $\kappa-\epsilon$ model by modifying the dissipation rate equations and turbulent kinetic energy²²⁾ and can accurately predict various flow regimes (including wall and free shear). The $\kappa-\omega$ model can handle complex flows with strong vortices and separation; however, its simulation results are significantly affected by the quality of the turbulence model constants and mesh, which makes it unsuitable for this simulation. The SST $\kappa-\omega$ turbulence model²³⁾ adopts the $\kappa-\omega$ turbulence model in the inner boundary layer, assumes the standard $\kappa-\epsilon$ model in the shear layer and boundary edge, and transfers the two models, but apparent turbulence will be generated. For this simulation, unsteady dynamic phenomena cannot be accurately analyzed and are unsuitable. The RNG $\kappa-\epsilon$ model is more efficient than the standard $\kappa-\epsilon$ model. The RNG $\kappa-\epsilon$ model suits for streamlined flow with rapid strain and large bends²⁴⁾. Based on the above analysis, the RNG $\kappa-\epsilon$ model simulates the external gear. The transport equation of the RNG $\kappa-\epsilon$ model is as follows.

4.2 Mesh processing methods

(1) Dynamic mesh

Complex flow patterns and hydraulic properties come into play during pump simulations, necessitating the use of a finer mesh. However, conventional CFD solutions often struggle with the challenges posed by rotating positive displacement mechanical systems. TwinMesh, a meshing tool developed by the German company CFX-Berlin, offers the capability to automatically generate high-quality hexahedral meshes for rotating positive displacement machinery. This approach enhances grid resolution, enabling a more precise description of the flow field, boundary layer flows, and gap flows while reducing oscillations and numerical dissipation. The use of high-quality hexahedral grids accurately represents complex geometries, mitigating issues related to shape distortions and node irregularities commonly associated with tetrahedral meshes. This, in turn, allows for a more accurate representation of flow direction and gradient. The parameter settings are as shown in Table 2 and the meshing results are shown in Figure 5.

Table 2 Main parameter table of TwinMesh.

Name	Value
Type of meshing	InnerFix
Maximum element size(mm)	2
Type of automatic mesh generation	Pre-/Post-Smoothing
Interface node mapping	Minimize distance
Fluid model	Incompressible

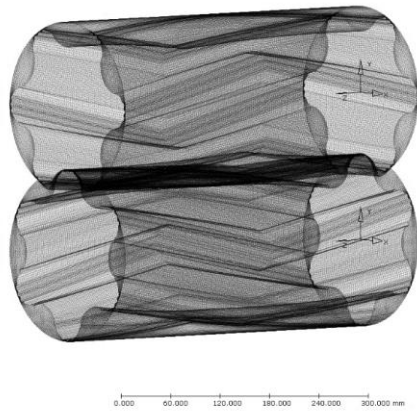


Fig.5 3D mesh of external herringbone gear pump rotors.

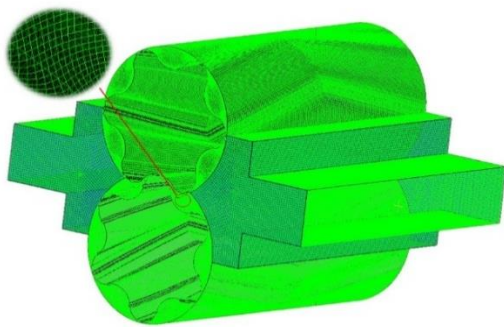


Fig. 6 Fluid calculation area for the external gear pump.

(2) Static mesh

For the non-rotating area (inlet and outlet), use ANSYS Meshing to obtain a static mesh, and sew the divided mesh with the mesh in the rotor area to obtain the fluid calculation area as shown in Figure 6. The boundary condition is shown in Table 3.

Table 3 Calculation condition parameter table.

Name	Value
Inlet pressure(bar)	1
Outlet pressure(bar)	10
Rotating speed (RPM)	300
Water density(kg/m ²)	998.2
Analysis type	Transient
Number of Timesteps per Run	20

5. Results and discussion

More detailed information can be obtained through CFD analysis methods (e.g., information that cannot be accepted by traditional experiments, such as fluid flow and heat transfer). The most important thing is visualization, which can help researchers understand fluid problems more vividly and help optimize design work. At the same time, the method discovers potential issues in advance and solves them in time. Many scholars have simulated external gear pumps using CFD. Frosina E

compared the model results with experimental data obtained on a dedicated test bench by the pump manufacturer and reported good consistency²⁵. Rana D used CFD to simulate the external gear pump, and the error range was within 5% compared with the experimental results²⁶. Therefore, CFD is an effective tool for analyzing the fluid characteristics of gear pumps²⁷.

5.1 Model validation and flow analysis

(1) Validation of results

The outlet flow rate was monitored, and after stable operation, the outlet flow rate was steady at 89.2kg/s. The calculated result is 92.87kg/s. The simulation results of the pump were lower than the theoretical displacement because side clearance will cause specific leakage and reduce the discharge volume. The error between the simulation and calculation results was 3.95%, so the model is valid, and the simulation results are credible.

(2) Flow analysis

Flow pulsation will cause significant fluctuations in outlet pressure and head. To directly obtain the pressure and head changes at the outlet. During the solution process, a monitor is set up to monitor and record the outlet pressure and head. The results are shown in Figure 7. According to Figure 7, after stable operation, the head range is 91.45 m – 91.80 m, with a maximum change rate of 0.38%; the outlet pressure range is 9.960 bar – 9.985 bar, with a total change rate of 0.25%. Therefore, the external gear pump has smaller flow pulsation and provides stable working pressure and lift.

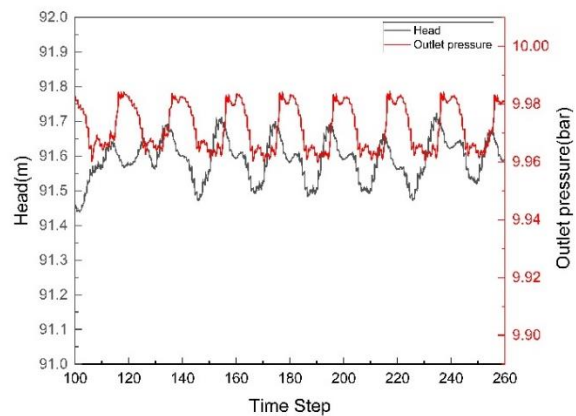


Fig. 7 Changes in head and outlet pressure of the external gear pump.

5.2 Analysis of pressure distribution

Obtain the pressure distribution cloud diagram of the XY center section at 0.333333 s, 0.366667 s, 0.4 s, and 0.43333 s in the same period (0.2 s), as shown in Figures 8 (a), (b), (c) and (d). The maximum pressure value is about 18bar. The isobars do not bend, intersect, or gather sharply in a particular area, and the pressure gradient is too gentle, so there is less chance of a pressure surge or

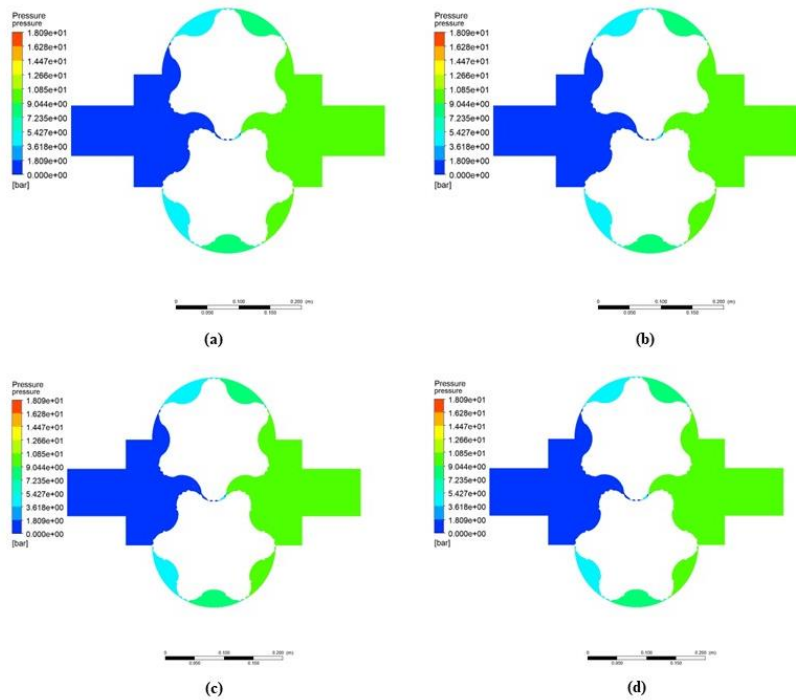


Fig. 8 (a) XY center plane pressure distribution at 0.333333s, (b) XY center plane pressure distribution at 0.366667s, (c) XY center plane pressure distribution at 0.4s, and(d) XY center plane pressure distribution at 0.433333s.

collapse point. It can be obtained from Figure 8 that as time changes, the overall internal pressure changes little, especially the pressure in the inlet and outlet areas is stable, so the internal flow is steady. The external gear pump operates smoothly and can provide stable pressure output and reduce the possibility of vibration and noise.

5.3 Axial force analysis

The magnitude of the axial force (Z-axis direction) experienced by the active rotor (R1) and the driven rotor (R2) is shown in Figure 9. During the start-up stage, due to the influence of unstable operation and liquid flow, the axial force on the main and driven rotors is relatively large. However, after stable operation, the force on the main and enslaved person rotors fluctuates around 0 N, close to 0. The main reason is that herringbone gears can effectively reduce or eliminate axial force but are affected by liquid flow during operation, causing changes in axial force. The design of the herringbone gear pump rotor can effectively reduce the impact of axial force on equipment operation and reduce friction and wear.

6. Conclusion

Rapid modeling using digital modeling methods facilitates the correction of various relevant parameters and, at the same time, lays the foundation for processing and CFD analysis. A comparison of the simulation results of the outlet flow and the theoretical displacement revealed an error rate between the calculation results and the simulation results of 3.95%. Therefore, the simulation results are valid. Through the analysis of the outlet

pressure and head, the numerical fluctuations are small (the maximum change rate is only 0.38% and 0.25%), which meets the design requirements of low-flow

pulsation. It can be seen from the pressure distribution cloud diagram form Fig.8 that because the isobars do not have sharp bends and intersections and the pressure gradient changes gently, the possibility of a pressure surge point or sudden drop point is low. At the same time, as time changes, the internal pressure of the pump body changes slowly, and the pressure in the outlet area is stable. Therefore, it can be judged that the operation is regular, and the outlet pressure output is sound.

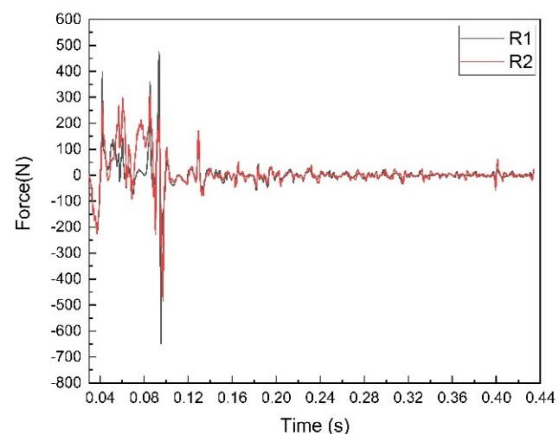


Fig.9 Rotor R1 and R2 axial force monitoring results.

Through the analysis of the axial force of the primary and driven rotors, the axial force is close to 0, which

reduces the wear on bearings and other components and extends the service life of the equipment. According to the above analysis results, the external meshing helical gear pump has slight flow pulsation, operates smoothly, and can provide stable pressure and lift. At the same time, the structure of the herringbone gear rotor solves the problem of sizeable axial force of the helical gear.

The gear rotor is an integral part of the gear pump, which will significantly impact the performance of a pump. On the other hand, the design of other components must be addressed. Therefore, the production of other features (such as sealing rings and water-retaining rings) will be the focus of subsequent research.

Acknowledgement

This research was supported by a grant(2023-MO IS35-005) of Policy-linked Technology Development Program on Natural Disaster Prevention and Mitigation on funded by Ministry of Interior and Safety (MOIS, Korea).

Conflicts of Interest

The authors have no relevant financial or non-financial interests to disclose.

References

- 1) Parker David B, "Positive displacement pumps-performance and application," Proceedings of the 11th International Pump Users Symposium. Turbomachinery Laboratories, Department of Mechanical Engineering, Texas A&M University, Houston, the US, pp. 137-140, 1994.
- 2) Elyamin, G. R. A., Bassily, M. A., Khalil, K. Y., and Gomaa, M. S, "Effect of impeller blade s number on the performance of a centrifugal pump," Alexandria Engineering Journal, Alexandria, Egypt, 58.1, pp. 39-48, 2019.
- 3) Kazama, T., Optimum Hydraulic Oil Viscosity Based on Slipper Model Simulation for Swash plate Axial Piston Pumps/Motors, Journal of Drive and Control, 18(4), pp.84-90, 2021.
- 4) Brinkmann, L., Kock, S., Lang, J., and Knoll, G, "Tribological analysis of the plain bearings in an external gear pump," IOP Conference Series: Materials Science and Engineering. Vol. 10 97. No. 1. IOP Publishing, Aachen, Germany, pp.1-11,2021.
- 5) Ransegnola, Thomas, Xinran Zhao, and Andrea Vacca, "A comparison of helical and spur external gear machines for fluid power application s: Design and optimization," Mechanism and Machine Theory, 142, 103604, pp.1-20, 2019.
- 6) Wang, W., Yin, Y. M., He, S. H., and Liu, G. M., "Study on flow characteristic of gear pumps by gear tooth shapes," Journal of Applied Science and Engineering, New Taipei City, Taiwan, 20.3, pp. 367-372, 2017.
- 7) Togashi, S., and H. Iyo, "The synthesis of tooth profile shapes and helical gears of high hydraulic performance for rotary type pumps," Mechanism and Machine Theory, 8.1, pp.105-123, 1973.
- 8) Liu, Dawei, Yanbo Ba, and Tingzhi Ren, "Flow fluctuation abatement of high-order elliptical gear pump by external noncircular gear drive," Mechanism and Machine Theory, 134, pp.338-348, 2019.
- 9) Xuegang, Zhang, and Liang Zheng, "Geometric Modeling and CFD Simulation of Curvilinear Cylindrical Gear Pumps," Iranian Journal of Science and Technology, Transactions of Mechanical Engineering, 47.1, pp. 1-17, 2023.
- 10) Zhao, Xinran, and Andrea Vacca, "Multi-domain simulation and dynamic analysis of the 3D loading and micromotion of continuous-contact helical gear pumps," Mechanical Systems and Signal Processing, 163, 108116, pp.1-28, 2022.
- 11) Park, J. W., Khan, H. A., Jeong, E. A., Kwon, S. J., Yun, S. N., & Lee, H. S, Pressure/Flow Pulsation Characteristics of the Hydraulic System for Behaviour Prediction of the Prefill Valve, Journal of Drive and Control, 18(2), 1-8, 2021.
- 12) Kong, F., He, Y., Zheng, D., Zhang, H., and Xia, B., "Analysis of influence factors on flow rate characteristics in gear pump," Journal of Drainage and Irrigation Machinery Engineering, 32.2, Jiangsu P.R. China, pp. 108-112, 2014.
- 13) LIU Kun, XU Lei, YANG Bo, Numerical simulation of external helical gear high-pressure pump with CFD[J]. Journal of drainage and irrigation machinery engineering(JDIME) ,2019,37 (4) : 307–312.(In Chinese).
- 14) Wu Yifei, Design of Double Circular Arc Helical Gear Hydraulic Pump and Analysis of its Axial Force[D]. Shandong University, 2020. (In Chinese)
- 15) Chen Lide, Basics of Mechanical Manufacturing Technology, Higher Education Press, Beijing, pp.106-113,2009.
- 16) Liu, Dawei, Yanbo Ba, and Tingzhi Ren. "Flow fluctuation abatement of high-order elliptical gear pump by external noncircular gear drive," Mechanism and Machine Theory, 134, pp. 338-348, 2019.
- 17) Huang, Kuo Jao, Wen Ruey Chang, and Wun Chuan Lian, "An Optimization approach to the displacement volumes for external spur gear pumps," Materials Science Forum. Vol. 594. Trans Tech Publications Ltd, 2008.
- 18) Li, Yulong, and Mao Tang, "Influence analysis of trapped oil pressure on flow pulsation in

- external gear pumps," Transactions of the Chinese Society of Agricultural Engineering, Beijing, P.R. China 29.20, pp. 60-66, 2013.
- 19) Yamaguchi, A, "Cavitation characteristics of long orifices in hydraulic systems," 5th international fluid power symposium, 1978.
 - 20) Del Campo, D., Castilla, R., Raush, G. A., Gámez Montero, P. J., and Codina, "Numerical analysis of external gear pumps including cavitation," Journal of Fluids Engineering, 081105, pp. 1-12, 2012.
 - 21) Choi, Y. H., Yoo, I. H., & Lee, C. H, Thermal Flow Analysis of an Engine Room using a Porous Media Model for Imitating Flow Rate Reduction at Outlet of Industrial Machines, Journal of Drive and Control, 19(1), pp.62-68, 2022.
 - 22) Habchi, C., Oneissi, M., Russeil, S., Bougeard, D., and Lemenand, T. "Comparison of eddy viscosity turbulence models and stereoscopic PIV measurements for a flow past rectangular-winglet pair vortex generator," Chemical Engineering and Processing-Process Intensification, 169, 108637, pp. 1-11, 2021.
 - 23) Menter, Florianr, "Zonal two equation kw turbulence models for aerodynamic flows," 23rd fluid dynamics, plasmadynamics, and lasers conference, Florida, U.S.A, 1993.
 - 24) Chen, Y., Wu, C., Wang, B., and Du, M, "Three-dimensional numerical simulation of vertical vortex at hydraulic intake," Procedia Engineering, 28, pp. 55-60, 2012.
 - 25) Frosina, Emma, Adolfo Senatore, and Manuel Rigosi, "Study of a high-pressure external gear pump with a computational fluid dynamic modeling approach," Energies, 10.8, 1113, pp. 1-20, 2017.
 - 26) Rana, Dipen, and Nirmal Kumar, "Experimental and computational fluid dynamic analysis of external gear pump," International Journal of Engineering Development and Research, 2.2, pp. 2474-2478, 2014.
 - 27) Shin, J., Pyo, J., Lee, M., Park, S., Park, S., Suh, J., & Jin, M, Hazardous Gas Detecting and Capturing Robot, Journal of Drive and Control, 19(2), pp.27-35,2022.